Climatic comparison between Belgium, Champagne, Alsace, Jura and Bourgogne for wine production using the regional model MAR

Sébastien Doutreloup, Benjamin Bois, Benjamin Pohl, Sébastien Zito, Yves Richard

OENO One
VINE AND WINE OPEN ACCESS JOURNAL
By iVES International Viticulture & Enology Society

DOI: https://doi.org/10.20870/oeno-one.2022.56.3.5356

OPEN ACCESS

ORIGINAL RESEARCH ARTICLE

Climatic comparison between Belgium, Champagne, Alsace, Jura and Bourgogne for wine production using the regional model MAR

Sébastien Doutreloup* [1,2], Benjamin Bois[1,3], Benjamin Pohl[1], Sébastien Zito[1] and Yves Richard[1]

[1] Centre de Recherches de Climatologie, UMR6282 Biogéosciences, CNRS / Université de Bourgogne Franche-Comté, Dijon, France
[2] Laboratory of Climatology, Department of Geography, SPHERES research unit, University of Liège, Liège, Belgium
[3] Institut Universitaire de la Vigne et du Vin, Université de Bourgogne, Dijon, France

*correspondence:
s.doutreloup@uliege.be

Associate editor:
João Santos

Received:
17 December 2021

Accepted:
6 June 2022

Published:
1st July 2022

ABSTRACT

In Belgium, vineyards have strongly increased over the last decades. Is it a trendy effect, or is Belgium becoming an increasingly favourable country for viticulture? A related issue is whether Belgium is similar to another French region from a climatic point of view. To address these questions, we use here the regional climate model MAR to provide high-resolution (5 km) climate information over the territory of Belgium and the north-eastern quarter of France. We first evaluate MAR outputs from a climate point of view against more than 150 weather stations and then from a viticulture point of view by computing bioclimatic indices, as well as key phenological dates and frost risk. The second step consists in comparing the four northernmost French wine regions (Champagne, Bourgogne, Jura and Alsace) with the Belgian wine region. MAR simulations are generally consistent with the observation, especially for the dates of the main phenological stages of the vine. Simulations of a frost risk in spring, heat stress in summer and Huglin's heliothermal index show slightly more disagreement, but biases remain moderate. The Belgium wine region appears to be quite comparable to the Champagne and Jura regions, despite colder conditions that influence its bioclimatic indices. Under current climate conditions, the main risk for Belgian vines is frost after bud break.t

KEYWORDS: Wine, Belgium, climate modelling, bioclimatic indices, phenology, hazards, frost risk

INTRODUCTION

In Europe, grapevines are mainly cultivated around the Mediterranean basin, as France, Spain and Italy account for 34 % of the world's vineyard area in 2020 (OIV, 2021). However, northern Europe has a long history of premium wine production, e.g., Mosel and Rheingau in Germany or Champagne and Burgundy in France. Recently, European countries that are not historical wine producers have been exhibiting rapid growth in the area devoted to vineyards (Jones and Schultz, 2016; Nesbitt *et al*., 2016). For example, Belgium has more than doubled the area dedicated to viticulture between 2011 and 2016, going from 119 ha to 300 ha (OIV, 2021) to reaching 587 ha in 2020, according to FGOV Economy (2021).

Due to global warming, isotherms shift towards higher latitudes and altitudes (IPCC, 2021; Nikulin *et al*., 2011). This is also true for Western Europe, where the annual temperature is projected to increase in a range of +1 °C to +5 °C depending on the climate models and greenhouse gas emission scenarios used (IPCC, 2021; RMI, 2020; Termonia *et al*., 2018). Such rapid warming implies that new regions will experience climate conditions more favourable to viticulture (Fraga *et al*., 2016; Moriondo *et al*., 2013). Hence, while wine production is and will probably be negatively impacted by global warming in some historical areas (Fraga *et al*., 2016; Resco *et al*., 2016), a collateral effect of global warming should be that northern European regions could be able to obtain more profitable wine production, in line with gains in cultivar diversity and/or modified vineyard distribution (Morales-Castilla *et al*., 2020).

The future wine-growing potential of northern temperate regions like Belgium should theoretically increase under a changing, increasingly warmer and yet more variable climate (IPCC, 2021; Seneviratne *et al*., 2021). Because of such long-term and ongoing changes, Belgium may have new grape growing and wine-producing regions. Before assessing and regionalizing possible evolutions of the climate in Belgium, climate variables that are relevant for viticulture should be selected, that is, those that most directly influence the yields and quality of wines. It is especially important to address the following two questions: (i) Do the current climate conditions in Belgium allow the cultivation of grapevines? (ii) Climatologically, could Belgium be considered a unique wine region, or does it show similarities with current nearby wine-growing regions such as Champagne or Bourgogne?

Addressing these questions requires high-resolution climate information that captures well the specificities of the terrain (including but restricted to topographic influence on atmospheric variables). These variables mostly consist of air temperature and humidity, as well as precipitation, under current and eventually future climate conditions. Thus, a regional climate model is needed to obtain spatially continuous and homogeneous data with a sufficient spatial resolution compatible with weak but potentially decisive topography. Despite the expected added value of these higher-resolution outputs upon coarser global models, the skill and biases of such a dataset need to be determined with great care, especially for all parameters (climate variables and derived indices) relevant to viticulture (Fraga *et al*., 2016; Remenyi *et al*., 2019). Motivated by this issue, the current study aims at (i) presenting a high-resolution modelling exercise devoted to these questions, using the so-called Regional Atmosphere Model (MAR), and (ii) evaluating the regional model outputs from a viticulture point of view.

The regional model is analysed with respect to observational data taken from meteorological stations over both current and renowned wine regions (namely, Champagne and Burgundy, in north-eastern France) and the targeted region whose wine-producing potential is to be assessed (namely, the Belgian territory). The model evaluation focuses first on the climate variables that influence grapevine and derived bioclimatic indices (such as the average, minimum, and maximum temperature during the growing season, the relative humidity that can influence the diseases of the vine, the precipitation on an annual scale, the heliothermal index of Huglin). It also considers hazards, both cold (spring frost) and hot (extreme temperatures during the summer) days, that can be detrimental to wine-growing possibilities. Finally, the MAR model is also evaluated on its ability to reproduce the dates of the different phenological stages of the vine (i.e., bud break, flowering, veraison, and maturity). Particular attention is paid to the phenological stage of maturity and sugar content to compare each region on its capacity to produce both still and sparkling wines.

This study is organized as follows. The following section presents the data, the definitions, and methods used in this work, including the climate settings of the regions, the numerical setup of MAR numerical experiments, and the bioclimatic and phenological indices relevant for viticulture. The next section is devoted to the presentation of the meteorological results, with detailed model evaluation performance compared to the weather stations from a climate (fundamental) point of view. After this evaluation of the MAR simulations, we detail a wine-growing (applied) approach based on model simulations to compare the current wine-growing regions. Finally, the last section provides a general conclusion and perspectives.

MATERIALS AND METHODS

1. Observational data and geographical regions

This study focuses on two distinct but neighbouring regions, namely Belgium (Figure 1A) and the north-eastern quarter of France (Figure 1B). The grid points included in the different viticultural regions are identified by a different colour in Figure 1. Each wine region is defined in the Vineyard Geodatabase (Bois *et al*., 2017) that has been rasterized on the MAR model grid resolution (about 5 km, see Section "Regional model and Setup"). Each wine production pixel corresponds to a location where an area with land cover classified as vineyards is found within the CORINE Land Cover 2012 database (CLC2012; (European Environment Agency, 2014)) in France.

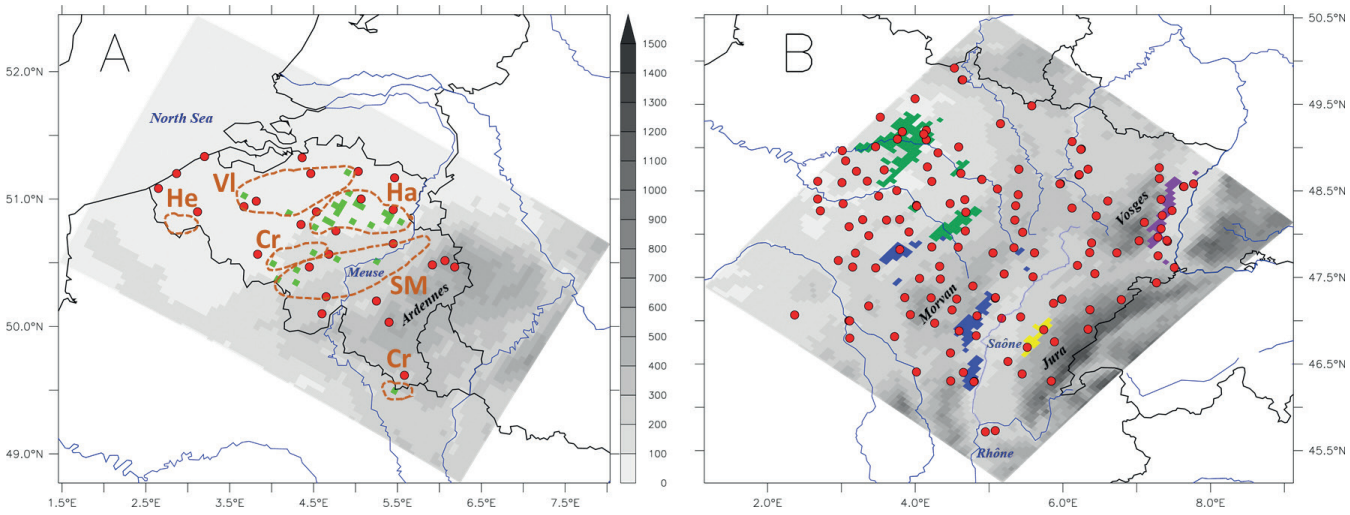

FIGURE 1. Model topography (greyscale in metres), location of the weather stations (red dots) used in this study and viticultural regions (in coloured pixels; light green: Belgium Wine Region (BWR), dark green: Champagne, blue: Bourgogne, yellow: Jura, purple: Alsace) on the domain covering Belgium (A) and on the domain covering the northeast quarter of France (B). The Protected Designation of Origin (PDO) or Geographical Indications (GI) of each BWR pixel is identified with dashed orange lines on map A with acronyms. He=Heuvelland; Ha = Hageland and Haspengouw; Vl = Vlaamse landwijn; SM = Côtes de Sambre et Meuse; Cr = Crémant de Wallonie (i.e., sparkling wine). Toponyms related to rivers and sea are in blue letters. Toponyms relative to the reliefs are in black letters.

For Belgium, vineyards do not cover sufficiently wide areas to be identified as such within CLC2012 or more recent versions. Hence, vineyard locations were identified within the Vineyard Geodatabase in 2016 through online research of actual wineries in Belgium and identifying nearby vineyards with Google Earth and Google Street view.

Each French wine region is named by its original name (i.e., Champagne, Bourgogne, Jura and Alsace). Belgium vineyards were named as a single wine region by the acronym BWR (for Belgium Wine Region). The corresponding Belgium Protected Designation of Origin (PDO) or Protected Geographical Indication (PGI) of each pixel is presented in Figure 1A (dark orange dashed lines): PDO Heuvelland, Hageland, Haspengouw, Crémant de Wallonie and Côtes de Sambre et Meuse and PGI Vlaamse landwijn.

The observational data used in this study come from two distinct observation networks of weather stations maintained by the weather services of Belgium and France. All data for Belgium come from 27 weather stations from the surface synoptic observation network (SYNOP) and all data for France come from 141 weather stations from the Météo France network, including (but not restricted to) SYNOP stations. The red dots in Figure 1 indicate each weather station used in this study, and Table S1 (in supplementary material) provides more detail on these observational networks. Note that, in Figure 1, the areas covered by the two domains are different (with north-eastern France larger than Belgium), but that the densities of the networks are comparable. The observational data used are daily mean, minimum and maximum temperatures, cumulative precipitation and relative humidity over 21 years (2000–2020). This period corresponds to the availability of data for the Belgian stations. Missing or erroneous data range from 0 % to 16 %, and stations with more than 20 % missing or erroneous data have been discarded (2 in Belgium and 7 in France).

2. Regional model and Setup

The regional model used in this study is the "Modèle Atmosphérique Régional" model (hereafter called "MAR") in its version 3.11.4. MAR is a three-dimensional atmospheric model coupled to a one-dimensional transfer scheme between the surface, vegetation and atmosphere (Ridder and Gallée, 1998). Initially, the MAR model was developed for the polar regions in both Greenland (Fettweis *et al*., 2013) and Antarctica (Kittel *et al*., 2018). It has also been successfully used for temperate regions such as Belgium (Fettweis *et al*., 2017; Doutreloup *et al*., 2019; Wyard *et al*., 2021). A complete description of this model is available in Kittel (2021).

Lateral boundary conditions are taken from the ERA5 reanalysis (Hersbach *et al*., 2020) every 6 hours and at a horizontal resolution of 0.25° (roughly 31 km). Forcing fields include air temperature, pressure, wind and specific humidity, as well as sea surface temperature. The spatial resolution of MAR is 5km over both Belgian (120 grid points × 90 grid points) and French domains (120 grid points × 110 grid points) shown in Figure 1. MAR outputs are archived at the daily timestep over the period 2000–2020. The comparison with observational data is based on the grid point nearest to each weather station.

3. Climate indices, phenological dates and statistical methods

In a first step, we focus on a climate-oriented evaluation of the MAR model against weather station observations. Each weather variable is extracted from the nearest MAR grid

point in elevation among the 9 nearest MAR grid points in the distance compared to the observation station. In a second step, we calculate regional indices for each of the five current wine regions to cross-compare them. For each step, three complementary levels of detail are addressed:

3.1. Annual and seasonal meteorological analysis

The comparison is first performed on an annual mean temperature and precipitation. A focus is made on the minimum spring (March to May) temperature and maximum summer (June to August) temperature, as the vine is sensitive to these two types of seasonal extremes, causing either frost or sunburn related damages (Huglin and Schneider, 1998). The simulations and observations are compared using two complementary metrics: the mean daily bias and the normalized root mean square error (RMSE).

3.2. Bioclimatic analysis for grapevine cultivation and wine production

To characterize the regional climate according to indices that directly influence the vine, a bioclimatic index inferring the potentialities for grapevines to produce ripe fruits for winemaking and two indices approximating the factors limiting yield are calculated.

The first one is Huglin's heliothermal index (Huglin, 1978), developed to estimate the potentialities for a given location to produce ripe grapes considering grapevine heat requirements. Huglin's index has been widely used to characterize wine-producing regions worldwide (Bois, 2020; Jones and Schultz, 2016; Tonietto and Carbonneau, 2004). It is also a potential indicator of the sugar content of grapes (Navrátilová *et al*., 2021).

$$\text{Huglin index} = K \sum_{01.04}^{30.09} max\left(0; \frac{T_{mean}+T_{max}-20}{2}\right)$$

where T_{mean} is the daily mean temperature and T_{max} is the daily maximum temperature; both temperatures with a baseline temperature of 10 °C; K is a parameter dependent on the latitude (e.g., $K = 1.02$ at 40° and $K = 1.06$ at 50°). At latitudes higher than 50° (like Belgium), K is defined by the formula proposed by Hall and Jones (2010). The Huglin index is calculated from April 1st to September 30th of each year. This index is applied to both observations and simulations for the sake of comparison.

The second and third indicators are the atmospheric frost ($T_{min} \leqslant 0$ °C at 2 m between March and June, a period hereafter referred to as "spring+") and intense atmospheric heat ($T_{max} \geqslant 35$ °C at 2 m between June and September, "summer+" hereafter) which are two factors that might damage grapevine tissues hence limiting grape production.

For these two indicators (frost and intense heat) based on thresholds, we use a contingency table (Table S2) to evaluate the simulation against the observations. From this Table S2, many indices can be calculated to evaluate the quality of the simulations. Below, we use three of them, namely, accuracy (fraction of correct simulation), probability of detection (fraction of observed cases that are well simulated) and success ratio (fraction of simulated events actually observed). They range from 0 to 1 (a perfect score is 1) and are calculated as follows:

$$\text{Accuracy} = \frac{hits+correctnegatives}{total}$$

$$\text{Probability of detection} = \frac{hits}{hits+misses} = \frac{hits}{observedyes}$$

$$\text{Success ratio} = \frac{hits}{hits+falsealarms} = \frac{hits}{simulatedyes}$$

The last indicator is the mean cumulative rainfall during the vegetative and ripening stages, from April to September. This indicator allows us to evaluate if there is enough precipitation (>200 mm) to prevent water stress but not too much (<400 mm) to avoid diseases linked to excessive precipitation, such as powdery and downy mildews (Bois *et al*., 2017; Gadoury *et al*., 2012; Gessler *et al*., 2011).

3.3. Phenological analysis

Four main phenological stages are considered "key" stages for the grapevine: (i) bud break, which corresponds to the emergence of green tissues (shoots) on the plant, i.e., the onset of vegetative growth (stage "C" according to the scale proposed by Baillod and Baggiolini, 1993), (ii) flowering (or stage "I"), (iii) veraison (stage "M"), when grape berries change colour and soften, i.e., the onset of grape ripening, and finally (iv) maturity (stage "N"), when the grapes are ready to be harvested.

As grapevine phenology is mostly driven by air temperature, phenological models make it possible to determine the Days Of the Year (hereafter called "DOY") when these stages are reached, depending on weather conditions and vine varieties. To estimate bud break DOY, we use here the combination of Smoothed-Utah (a model based on dormancy rise chilling units; Bonhomme *et al*., 2010) and Wang and Engel (a curvilinear heat units model; Wang and Engel, 1998) that Morales-Castilla *et al*. (2020) adapted for many grapevine cultivars. This model is hereafter referred to as the SUWE model (for Smooth-Utah Weng and Engel). DOYs for flowering and veraison were simulated with the GFV model (Parker *et al*., 2011).

The last key stage is "maturity". Ripeness is a concept that changes according to the type of product. During the ripening process, sugar accumulates in grapes and acidity levels fall. Depending on the expected final product, grapes might be harvested with changing levels of sugar concentration. For sparkling wines, grapes are harvested with approximately 170 g/L of sugar concentration. For still wine, riper grapes are sought (typically from 200 to 240 g/L). To estimate DOYs for a "theoretical maturity" stage, we used the GSR model (Parker *et al*., 2020), a linear degree-days model with a base 0 °C temperature, starting on DOY 91, to simulate the date at which a sugar concentration of 200 g/L in grapes is reached (which provides, after fermentation, at wine with approximately 11.9 % vol. of alcohol).

Here, all indicators are computed with parameters for the grapevine cultivar Chardonnay. Chardonnay is the main

cultivated white variety in Burgundy and Champagne and represents more than 4 % of the total share of cultivated cultivars worldwide (Anderson and Aryal, 2013). Parameter values for each model used are shown in Table S3.

A comparison of the obtained dates is made between the observed and modelled data. For this comparison, two statistical criteria are used: RMSE and the model efficiency index (EF), according to Nash and Sutcliffe (1970).

$$EF = 1 - \left(\frac{\sum_{i=1}^{n} (S_i - O_i)^2}{\sum_{i=1}^{n} (O_i - \bar{O})^2} \right)$$

where O_i is the observed value, S_i is the simulated value, $\bar{O}$ is the average of observed values, and n is the number of observations. EF values range from $-\infty$ to 1 and a perfect score is 1.

Another index directly dependent on the bud break DOY is considered. While grapevine wintering tissues can resist cold down to –25 °C (Ferguson *et al*., 2011), after bud break, grapevine tissues can no longer tolerate freezing conditions. Then finally, to further assess the risk of frost damage, we also compute the percentage of years with at least one frost day occurring after the simulated bud break and before late July due to the very strong sensitivity of grapes to frost events during this phenological stage.

For clarity, all weather variables or indicators announced above and the questions they address are summarised in Table S4.

RESULTS AND DISCUSSIONS

1. Climate-oriented evaluation of MAR simulations

In this Section, we analyse some meteorological variables or indicators that directly influence grapevine cultivation. The main objective is to assess how these variables or indicators behave spatially, but also to identify the strengths and weaknesses of the MAR simulations.

1.1. Annual and seasonal meteorological evaluation

The mean annual temperatures (Figure S1) and precipitation (Figure S2) are strongly dependent on the topography. In Belgium for the period 2000–2020, mean annual temperatures range from 12 °C at the coast to 7 °C in the Ardennes, while precipitation ranges from 600 mm/year at the coast

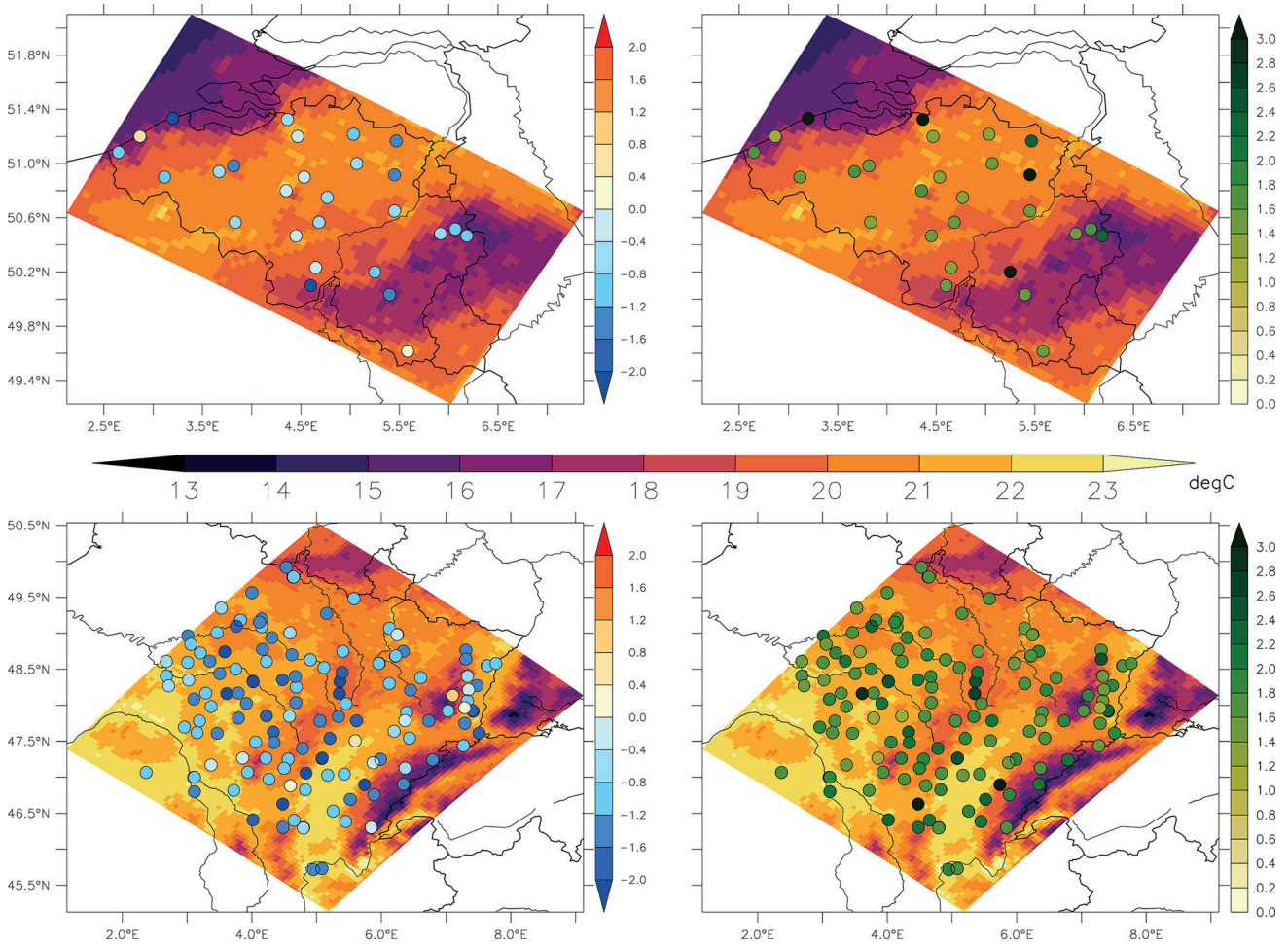

FIGURE 2. Mean summer maximum temperature in °C (background map and central colour scale) simulated by MAR. Mean summer maximum temperature biases (left, in °C) and RMSE (right, in °C) of MAR simulations compared to weather observations over the Belgian (upper) and French (lower) domains during the period 2000–2020.

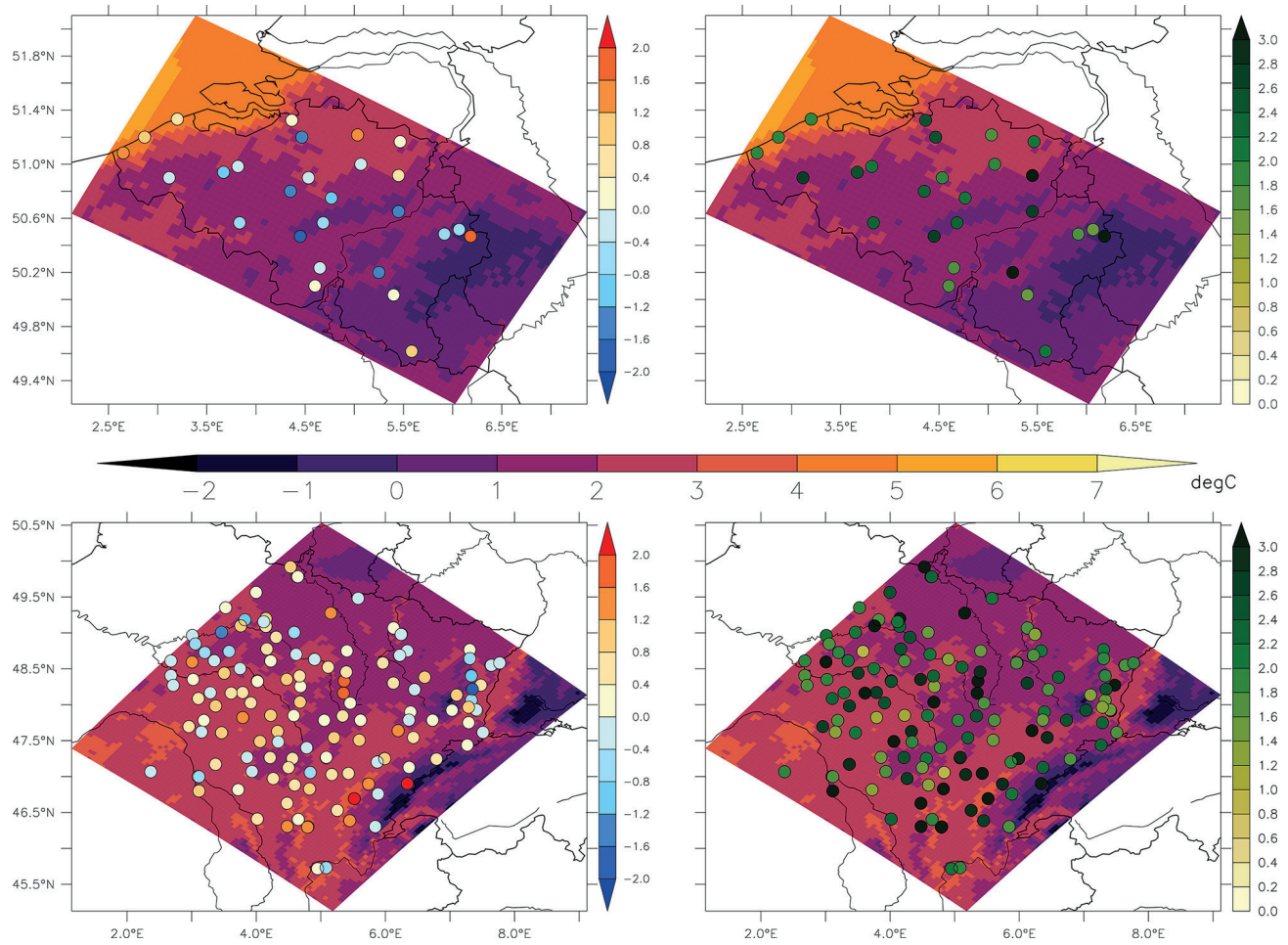

FIGURE 3. Mean spring minimum temperature in °C (background map and central colour scale) simulated by MAR. Mean spring minimum temperature biases (left, in °C) and RMSE (right, in °C) of MAR simulations compared to weather observations over the Belgian (upper) and French (lower) domains during the period 2000–2020.

to 1400 mm/year in the same regions, respectively. In the north-eastern quarter of France, the corresponding mean temperatures range from 13 °C in the Rhône Valley near Lyon to 6 °C in the Vosges and Jura mountains. Precipitation ranges from 550 mm/year in the Champagne region (near Reims) and in the Rhône valley to 1400–1900 mm/year over the Vosges and Jura mountains.

Except for some specific stations, the MAR model performs rather well in simulating these variables. For temperatures, the comparison between MAR simulations and observation stations shows a bias between –0.8 °C and 0.8 °C for both the Belgian and French domains. The RMSE of mean annual temperature is slightly larger in Belgium (with 1.6 °C) than in France (1.4 °C). For precipitation, the average daily bias is between –0.4 mm/day and 0.8 mm/day, giving an average RMSE of 1.8mm/day. These results are quite comparable to those obtained over Burgundy by another regional model for both temperature and precipitation (Boulard *et al.*, 2016; Marteau *et al.*, 2015).

These annual values conceal marked differences over the year. In summer in Belgium, the lowest maximum temperatures are found along the coast (~15 °C) and in the Ardennes (with 13 °C), while elsewhere, the maximum summer temperature is around 20 °C (Figure 2). Over the French domain, the lowest maximum temperature is located on the reliefs of the Vosges and the Jura (14 °C), but also, to a lesser extent, on the Langres plateau and the Morvan hills (16 °C). Elsewhere, it is around 23 °C, and even higher in the south of the domain. Over both domains, the MAR simulations underestimate the maximum summer temperature. Except for a few stations (where they can exceed 3 °C), RMSEs are typically between 1.4 and 1.8 °C (Figure 2), which remain equivalent to the annual values.

In spring, observed minimum temperatures in Belgium vary between +5 °C (along the coast) and –1 °C (summits of the Ardennes), as shown in Figure 3. In France, springtime conditions are milder in the Saône valley and on the Parisian Plateau (+3 °C) and colder on the highest reliefs (<-2 °C). The statistical indicators for spring minimum temperatures are more variable than for summer maximum temperatures. In Belgium, the MAR simulations underestimate the minimum spring temperatures in 56 % of the stations, while in France, MAR overestimates it in 66 % of the stations. Corresponding RMSEs in both domains (2.3 °C on average) are higher than the RMSE of the annual mean temperature observed, thereby indicating a lower skill.

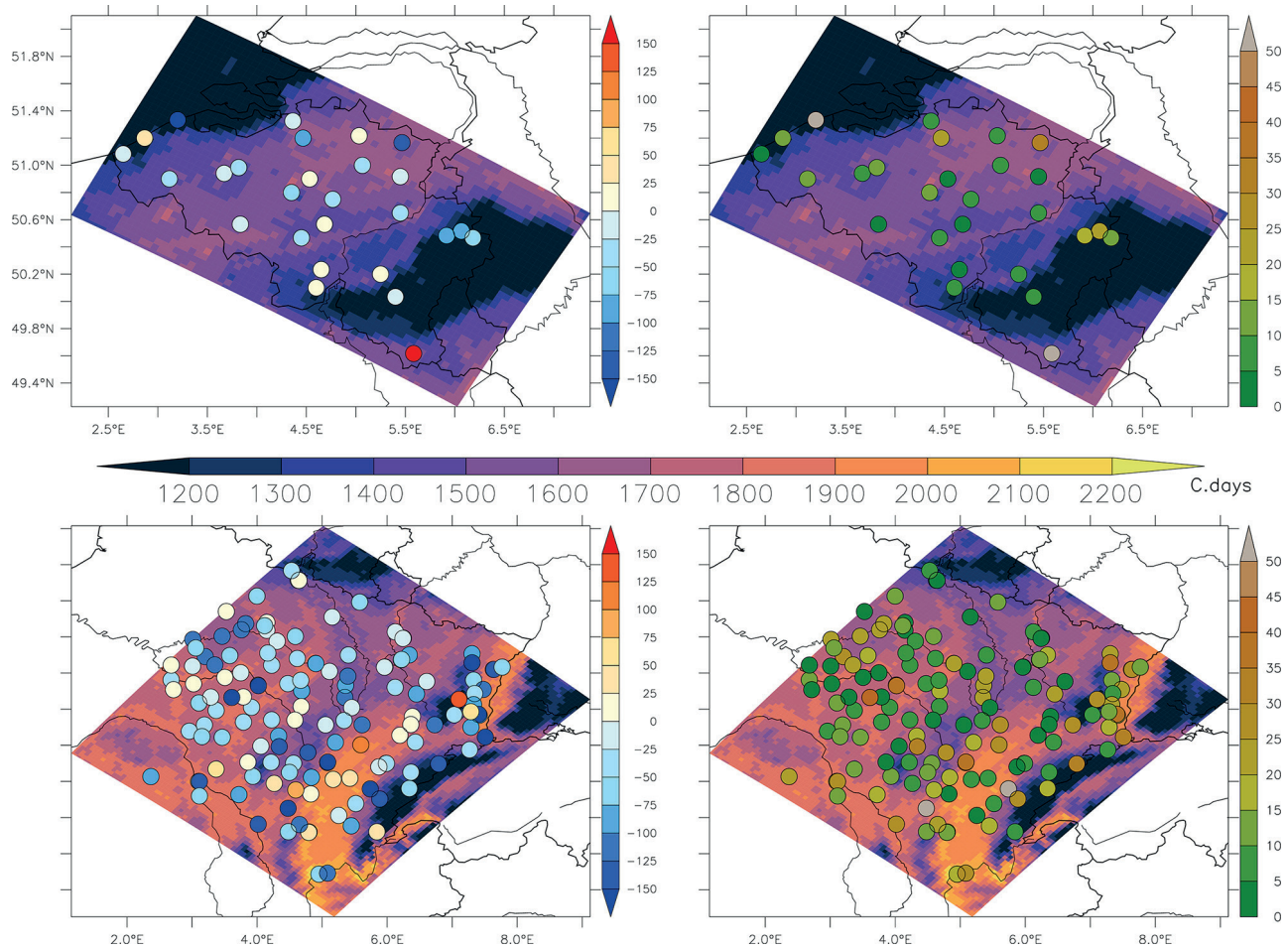

FIGURE 4. Mean annual Huglin index (background map and lower colour scale in °C.days) for Belgian domain (upper) and French domain (lower) simulated by MAR model simulations (middle) during the period 2000–2020. The round points represent the biases (left, in °C.days) and the RMSE (right, in °C.days) of the Huglin indices between the MAR simulations and the observations at weather stations.

In summary, the meteorological variables influencing the vine are primarily driven by the topography and, secondly, by the distance to the sea (especially for the Belgian domain). The MAR simulations are generally in good agreement with observed mean temperature and precipitation. However, summertime maximum temperatures are underestimated in both domains and the springtime minimum temperatures are mainly underestimated in Belgium and overestimated in France. Similar biases have been reported by previous studies using other models, like Xu *et al*. (2012) over Burgundy, Hamdi *et al*. (2015) over Belgium or Nikulin *et al*. (2011) with several RCMs over the whole of Europe. Possible causes involve potential biases inherited from the forcing GCMs (Xu *et al*., 2012) or question the representativeness of the model grid-points against much more complex and anisotropic surface conditions in the real world (Nikulin *et al*., 2011).

1.2. Bioclimatic indices-based evaluation

Figure 4 displays the spatial variability of the Huglin index. In Belgium, following the spatial distribution of air temperature, the Huglin index shows higher values between the coast and the Ardennes, where the values are quite low (<1300 °C.days). Values exceed 1600 °C.days along the Meuse valley and even >1700 °C.days in northern Belgium and the Lille area. In the French domain, the highest values (>1900 °C.days) are found along the Saône and Rhône valleys; the lowest values are in the highlands. For the rest of the domain, the values are higher than in Belgium and range from 1600 to 1900 °C.days.

A common characteristic of both domains is that the simulations underestimate the Huglin index values overall (mean biases for Belgium is –36 °C.days and –50 °C.days for France). RMSE values are also comparable between the two domains, with mean values of 14–15 °C.days. These biases in the simulated index are largely due to underestimations of summertime maximum temperature (Figure 2); this period contributed to most of the accumulation of degree days integrated into the calculation of the index (Section "Climate indices, phenological dates and statistical methods"). This negative bias for the Huglin index has already been observed over Croatia for many RCM participating in the EURO-CORDEX modelling exercise (Omazić *et al*., 2020). Similar results have been mentioned for Europe using the COSMO-CLM regional climate (Malheiro *et al*., 2010).

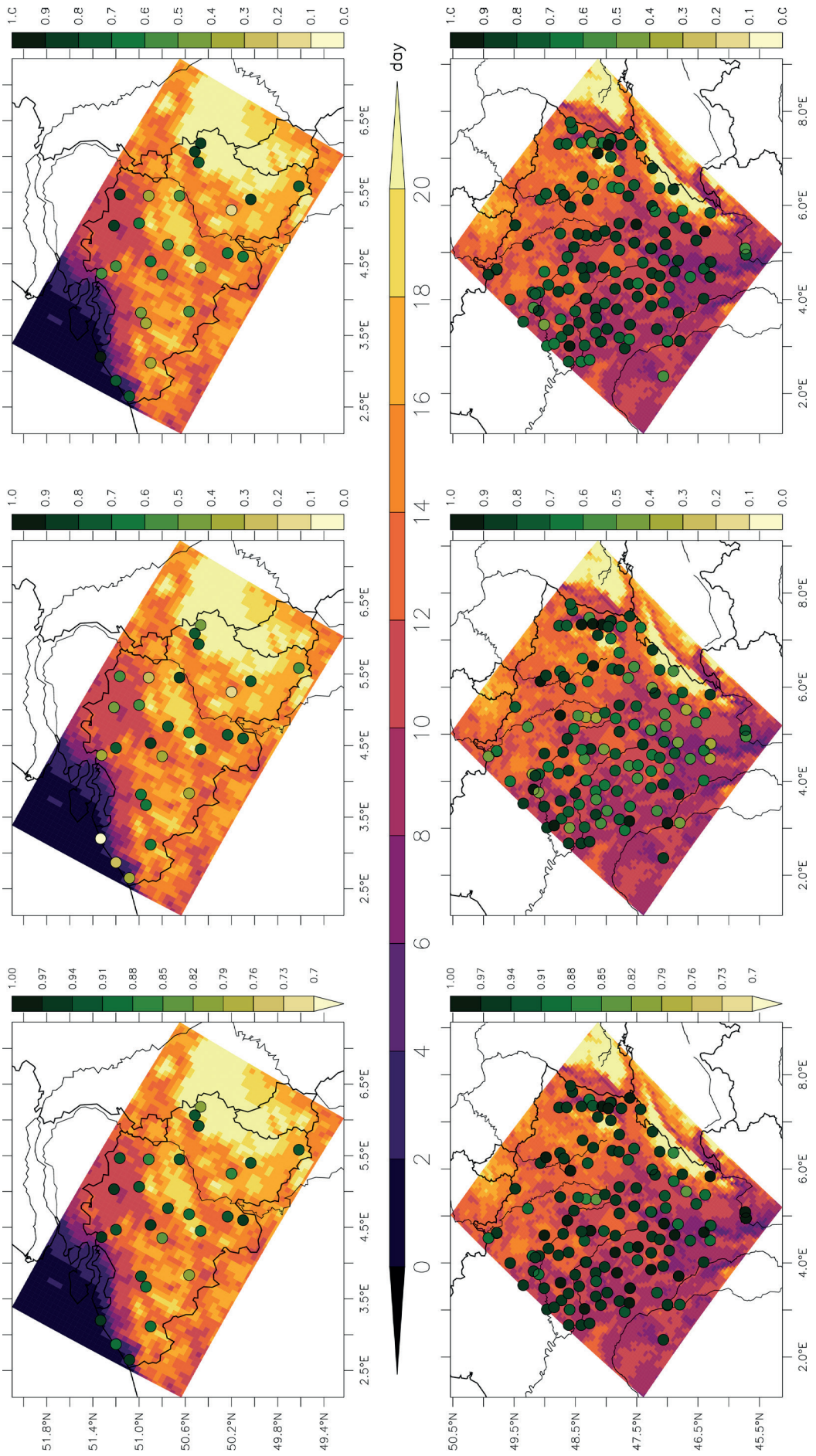

FIGURE 5. Mean number of spring+ frost days $T_{min} \leq 0$ °C (background map and middle colour scale in the day) for Belgian domain (upper) and French domain (lower) simulated by MAR simulations during the period 2000–2020. The round points represent the accuracy (left, no unit), the probability of detection (centre, no unit), and the success ratio (right, no unit) of the frost day between the MAR simulations and the observations at weather stations.

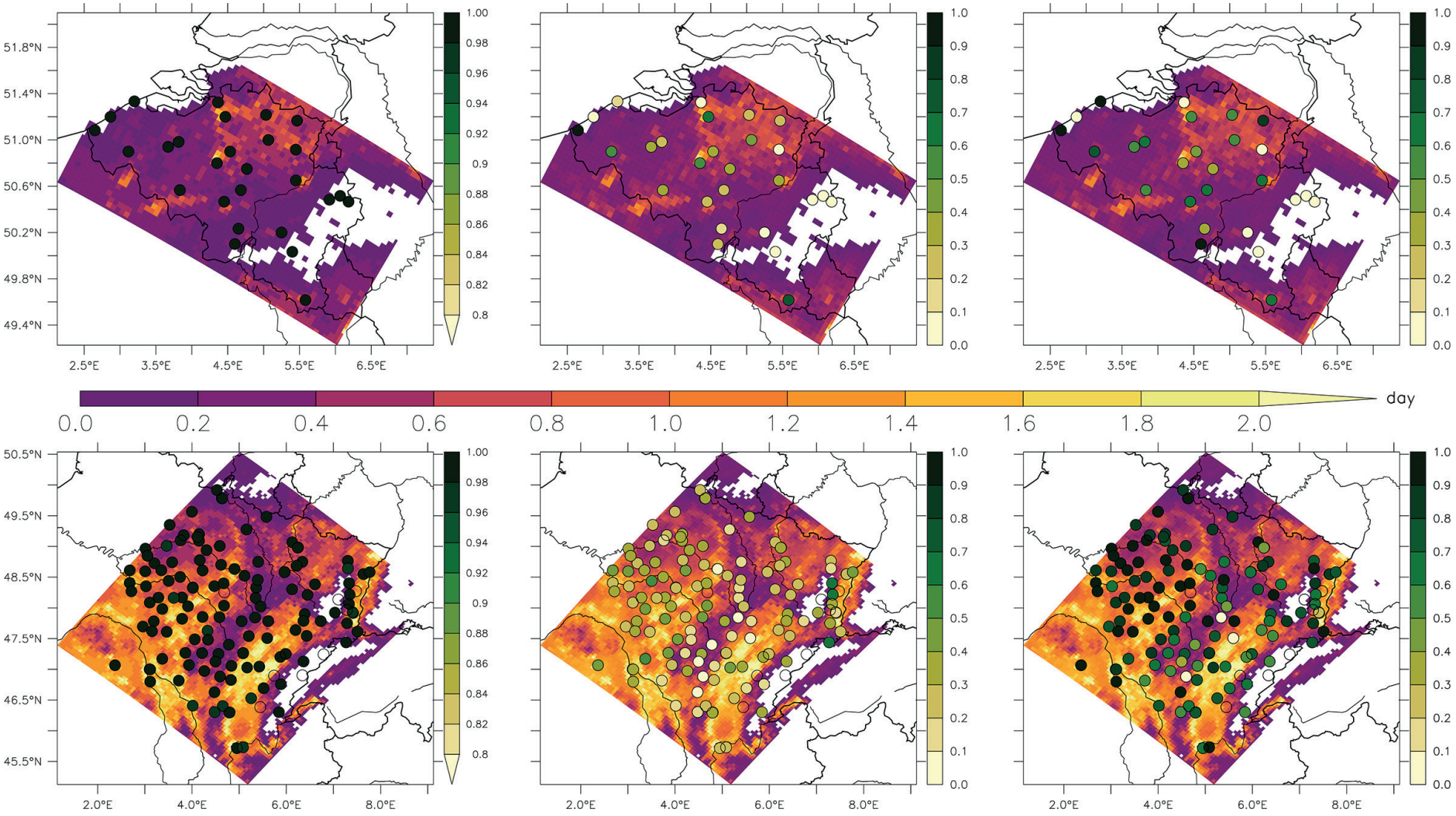

FIGURE 6. Mean number of summer+ hot days $T_{max} \geq 35$ °C (background map and middle colour scale in day; White areas mean there is no day ≥35 °C during 2000–2020) for Belgian domain (upper) and French domain (lower) simulated by MAR simulations during the period 2000–2020. The round points represent the accuracy (left, no unit), the probability of detection (centre, no unit), and the success ratio (right, no unit) of the number of summer+ hot days between the MAR simulations and the observations at weather stations.

As expected, spring+ frost days (shown in Figure 5) are obviously more frequent in elevated regions. During spring+, they are more frequent in Belgium than in the north-eastern quarter of France, thereby depicting the mean zonal gradient. Except for a few erratic stations, the three metrics used to compare simulations and observations show quite high values in both Belgium and France. The percentage of accurate simulations there is 91 % and 94 %, respectively. The percentage of observed frost days compared to simulated ones is 59 % for Belgium and 70 % for France. Finally, the percentage of simulated frost days compared to observed events are, respectively, 61 % and 77 %. These percentages indicate that MAR simulates frost days correctly in ~60 % of the cases in Belgium and that it simulates them even better for the French domain in more than 70 % of the cases.

Symmetrically, hot days (Figure 6) are more frequent in the French domain than in Belgium. In Belgium, the coast and the Ardennes rarely experience hot days so far. The rest of the country experiences between 0.5 and a little more than 1 hot day per year. Similar proportions are found in the north of France, but elsewhere hot days are much more frequent (more than 2 up to a maximum of 7 hot days per year, depending on the region). MAR simulations produce a number of hot days equivalent to those found by (Fischer and Schär, 2010).

The skill of MAR simulations is sensibly weaker than for frost days. The proportion of observed hot days that were well-simulated drops to 36 % for Belgium and 30 % for France. The fraction of simulated hot days currently observed is 60 % (Belgium) and 79 % (France). The percentage of good simulations (99 % for both domains) is less meaningful here due to the few cases available over the period. The skill is better for large-scale events (fraction of simulated currently observed), probably because they are at least partly forced laterally along the domain boundaries of the model, while finer-scale events (fraction of observed events well simulated) show a larger stochastic component.

Finally, the mean cumulative precipitation during the active vegetation stages (i.e., April through September) is shown in Figure S3. Both biases and RMSE of these rainfall totals are quite low for both domains, denoting a good estimation of precipitation: the Belgian domain has a mean bias of -0.05 mm/day and an RMSE of 2.5 mm, while the French domain has a mean bias of -0.09mm/day and a mean RMSE of 2.3 mm.

1.3. Phenological/theoretical maturity evaluation

The central colour (green) of Figure 7 shows regions with a theoretical maturity of the Chardonnay cultivar (with 200 g/L of sugar concentration) that occurs between September 10th (DOY > 255) and October 20th (DOY < 295) of each year. This allows for the delineation of the areas favourable to this cultivar. DOY values below 255 (pink colour in Figure 7) indicate an early theoretical maturity, which does not discard grapevine cultivation, but might be challenging, specifically in a context of a warming climate, because the ripening process might lead to very high alcohol and low acidity (Jones *et al*., 2005; van Leeuwen and Darriet, 2016; Madelin *et al*., 2010). By contrast, DOY values above 295 (purple colour in Figure 7) denote a late theoretical maturity, indicating, therefore, that the grape is not mature enough to be harvested in time.

Figure 7 shows that, based on maturation criteria, cultivation of Chardonnay is theoretically possible everywhere in Belgium, except over the main reliefs. Concerning the French domain, the theoretical maturity is also optimal over most of the territory, apart from the relief. In the Rhone and Saône valleys, theoretical maturity for this variety is too early (before September 10th).

Except for a few scattered weather stations, the performance of the MAR model to determine the DOY of the theoretical maturity for still wines (as evaluated by the efficiency) is 0.74 over the Belgian domain (except for the high reliefs) and is 0.66 for the French domain, indicative of good efficiency (Table S5). Similar performance has been obtained using the GSR model for Bordeaux red grapes varieties (Bois *et al*., 2018). The mean RMSE of theoretical maturity is 4.62 for Belgium and 4.77 for France (Table S6), also suggesting a good fit of the MAR model compared to weather observation.

The other phenological stages of the cultivar Chardonnay even show better EF values for flowering and veraison stages but lower ones for bud break (Table S5). Corresponding RMSE is also better for flowering and veraison stages but higher for the bud break stage in the Belgium domain (Table S6).

As shown in Table S7, the mean biases for each phenological stage are positive for the Belgian domain and do not exceed +4.4 days (bud break stage), except for the maturity, which has a negative bias of –0.2 days. In the French domain, the biases are positive and below +2.8 days (bud break stage), except for maturity, which has a negative bias of –2.5 days. Hence, both the Belgian and French domains show similar biases, which are higher for the bud break and lower for the other stages.

Overall, MAR simulates phenological stages with rather a good accuracy ($0.40 < EF < 0.79$, $2.39 < RMSE < 5.50$ and $-2.50 < Bias < 4.40$). However, the bud break phenological stage is almost systematically associated with the poorest scores. This is probably because the method used to determine this stage accumulates a much larger number of days before reaching the stage threshold than the other stages. Thus, the bud break stage has a much larger cumulative error which is reflected in the results but which remains comparable to the values found in other studies (Bois *et al*., 2018).

2. Climatic and bioclimatic indices spatial comparison

In this section, we calculate these indicators specifically for each wine region defined in Figure 1. The data of all grid points of a given wine region are averaged to obtain a regional index, allowing them to cross-compare these regions. In this section, only the values obtained by the MAR simulations are used as there are too few weather stations to be representative of these regions.

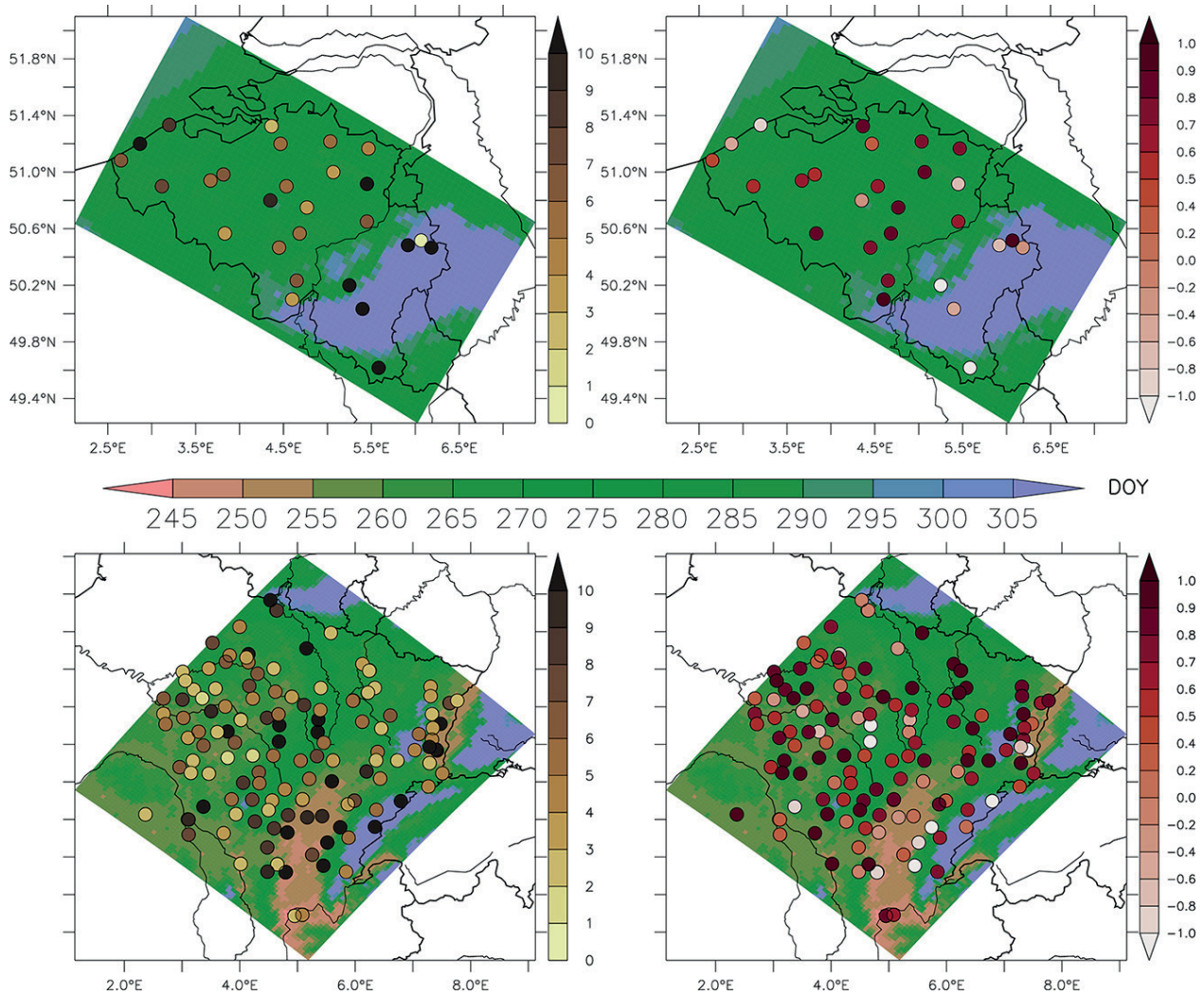

FIGURE 7. The background map and middle colour scales show the Day Of the Year (DOY) of the theoretical maturity for still wines (200 g/L of sugar concentration) of the cultivar Chardonnay for the Belgian domain (upper) and French domain (lower) simulated by MAR simulations during the period 2000–2020. The round points represent the model efficiency index (right, no unit) and RMSE (left, in DOY) for each stage with respect to the observations at weather stations.

2.1. Annual and seasonal comparison

Table 1 shows a comparison of some meteorological variables averaged over the five regions currently planted with grapevines. The Belgium Wine Region (BWR) generally shows colder mean annual and seasonal temperatures than all French regions. However, BWR is equivalent to Champagne and almost to Jura for the mean annual maximum temperature and equivalent to the Jura for the mean summer maximum temperature. It should also be noted that the BWR has more abundant annual rainfall than Champagne, Bourgogne and Alsace but largely less mean annual rainfall than the Jura.

However, comparing the differences between the wine regions with the magnitude of the biases and RMSE of the MAR model (shown to be of weak to moderate magnitudes: see Section "Climate-oriented evaluation of MAR simulations") leads us to conclude that the annual and seasonal temperature of BWR cannot be considered as significantly different from those of the French viticultural regions. This result holds for precipitation, with annual biases and RMSEs larger than the differences between BWR and the French wine regions (except for the very wet Jura wine region).

2.2. Bioclimatic indices-based comparison

According to Huglin's heliothermal index, BWR shows the lowest value among the wine regions considered (Table 2). The Huglin indices for other regions exceed 1650, giving an extra 150 degrees.days compared to BWR (barely exceeding 1500). According to Tonietto and Carbonneau (2004) classification, bioclimatic conditions are "cool" (>1500 and ≤1800 °C.days) for BWR, Jura and Champagne, and temperate (>1800 and ≤2100 °C.days) for Bourgogne and Alsace. Even when considering the biases and RMSEs discussed in Section "Climate-oriented evaluation of MAR simulations", the BWR remains the region with the lowest Huglin's index value, although falling in the same class as Champagne and Jura in the Tonietto and Carbonneau (2004) viticultural climate classification.

TABLE 1. Comparison of the 2000–2020 average meteorological values (mean annual precipitation, mean annual temperature, mean annual/summer maximum temperature, mean annual/spring temperature) simulated by MAR model forced by ERA5 reanalysis for the five regions currently planted with grapevines.

	Mean annual precipitation (mm/year)	Mean annual temperature (°C)	Mean annual maximum temperature (°C)	Mean summer maximum temperature (°C)	Mean annual minimum temperature (°C)	Mean spring minimum temperature (°C)
Bourgogne	766	11.6	15.5	21.9	7.7	2.6
Champagne	727	11.8	14.8	20.9	7.2	1.8
Jura	1339	10.9	14.7	20.1	7.0	2.3
Alsace	614	11.4	15.6	21.9	7.0	1.9
Belgium Wine Region	827	10.2	14.8	20.0	6.3	1.3

TABLE 2. Comparison of the 2000–2020 average viticultural values: Huglin index, mean spring temperature, mean spring+ frost day ($T_{min} \leq 0$ °C), mean summer+ temperature, mean summer+ hot day ($T_{max} \geq 35$ °C) and mean cumulative precipitation between April and September simulated by MAR model forced by ERA5 reanalysis and averaged over the five regions currently planted with grapevines.

	Huglin's heliothermal index	Mean spring temperature (in °C)	Mean spring+ frost day (in day)	Mean summer+ temperature (in °C)	Mean summer+ hot day (in day)	Mean cumulative precipitation between April to September (in mm)
Bourgogne	1865	6.1	9.0	17.5	1.3	229
Champagne	1695	5.6	11.5	16.6	0.6	244
Jura	1678	5.3	11.3	16.2	0.8	415
Alsace	1914	6.0	12.8	17.5	1.7	235
Belgium Wine Region	1511	4.9	15.8	15.5	0.4	258

Table 2 also shows that the BWR experiences the lowest mean spring temperature (4.9 °C) and the highest average number of frost days (15.8 days), while the French wine regions are warmer and range from 5.3 °C (for Jura) to 6.1 °C (for Bourgogne) and from 9 frost days (for Bourgogne) to 12.8 frost days (for Alsace). The differences between the minimum spring temperatures of all wine regions are smaller than the average RMSE obtained in Belgium and France. This leads us to conclude that the mean spring temperature of BWR cannot be considered significantly different from those of the French viticultural regions. Concerning the number of frost days, the Section "Climate-oriented evaluation of MAR simulations" indicates that the accuracy of the MAR model on this variable is higher than 90 % for both domains. Therefore, even with a 10 % inaccuracy, BWR remains the region with the highest number of frost days in spring+.

The BWR also experiences the coolest conditions: 15.5 °C for the summer+ mean temperature and 0.4 mean summer hot days, while the French regions range from 16.2 °C for Jura to 17.5 °C for Bourgogne and Alsace and from 0.6 hot days for Champagne to 1.7 hot days for Alsace. When comparing these values to the errors obtained in Section "Climate-oriented evaluation of MAR simulations", it can be seen that the differences between BWR, Jura and Champagne are smaller than the RMSE of the mean summer+ temperature. However, the mean summer+ temperatures for Bourgogne and Alsace are significantly warmer than the three other viticultural regions. Concerning the hot days, the comparison between regions and also between MAR and observations is less robust due to the relative rareness of these events, raising thereby the question of the sample sizes. Nevertheless, BWR, Jura and Champagne seem to show quite similar values compared to the other two regions.

Finally, Table 2 shows that the BWR region shows mean April to September precipitation amounts slightly larger (258 mm) than Bourgogne (229 mm), Alsace (235 mm) and Champagne (244 mm) but more than 150 mm lower than the Jura (415 mm). Concerning the biases and RMSE, the BWR experiences April to September precipitation equivalent to Alsace, Champagne and Bourgogne, and these four regions are all drier than the Jura region. These results are coherent with a worldwide analysis of average precipitation for the early 21st century that indicates that April to September precipitation typically reaches 230 mm for Southern Europe against 426 mm for Northern European wine-producing regions (Bois, 2019).

To sum up, the BWR region exhibits the lowest mean value of Huglin's heliothermal index compared to the 4 French viticultural regions. BWR also experiences more spring+ frost days and colder mean summer+ temperature. The inter-comparison of the number of hot days is more uncertain. BWR has a mean spring + temperature equivalent to Champagne and Jura and April to September precipitation amounts similar to those of Champagne, Alsace and Bourgogne.

2.3. Phenological comparison

BWR is the region where the DOY of each phenological stage occurs latest: when compared to other regions, this leads to a shift of +5 to +8 days for bud break, +5 to +11 days for flowering, +10 to +19 days for veraison and +14 to +27 days for maturity (Table 3). Even when considering the model errors (Tables S5, S6 and S7), BWR shows a significant delay since the calculation of these DOY is based on cumulative temperature, which is lower in BWR than in the other regions of France. In practice, these DOYs correspond well to the dates observed in the field (e.g., mean harvest date at DOY 255 in the Beaune area in 2000–2018: Labbé *et al*. (2019)), specifically for the maturity stage where the DOYs simulated by MAR seem close to the observations.

Table 3 further indicates that, under current climate conditions, all the wine regions studied here reach grape maturity before October 31st of each year. Hence, the risk of not reaching maturity with the Chardonnay cultivar is null.

Finally, the percentage of years with frost occurring after bud break (Table 3) clearly shows non-negligible differences between BWR and other viticultural regions. Frost risk there would be about (or more than) twice that recorded in French regions, except Jura, a difference that is much larger than modelling errors. Thus, BWR is a more risky region regarding frost after bud break. Nevertheless, it is worth noting that the minimum spring temperature is mainly underestimated over the Belgium domain, suggesting that the number of frost days could be overestimated.

Hence, the BWR can be considered a later wine region than the four regions of the French domain. Although later by almost a month than Alsace, for example, the theoretical maturity (200 g/L) of Chardonnay simulated in Belgium occurs before October 31st during the whole study period. Therefore, BWR has no risk of not being harvested. However, the risk of frost after bud break is 14 % to 29 % higher in BWR than in other French regions.

3. Wine potential of Belgium

Historically, even taking into consideration the advantage of longer days during summer at high latitudes, agronomists considered that grape production would be very limited over a limit roughly defined in Europe as around 50°N (Huglin and Schneider, 1998). The very fact that the day length "k" factor in Huglin's Heliothermal index was parameterized for latitudes equal to or below 50°N. Huglin and Schneider (1998) show that wine grape cultivation was not seriously considered elsewhere before the 21st century. Yet, using the updated version of "k" as proposed by Hall and Jones (2010), Huglin's index reaches values over 1500 °C. days for most of the Belgium territory (Figure 4). This index classifies Belgium vineyards as "very cool", for which very early varieties are adapted. Regions for still and late harvest wine production, such as Geisenheim in Germany (49,99 °N where Johannisberg winery producing wine since the 8th century) or Vaud region close to Geneva in Switzerland (latitude 46.37 °N) or sparkling white wines such as Champagne was classified in this group when considering 1961–1990 climate conditions (Tonietto and Carbonneau, 2004). Within Belgium, the Hageland (Brabant province) and Haspeng (Limburg province, "Ha" on Figure 1A) exhibit higher Huglin index values (Figure 4), in comparison to Côtes de Sambre et Meuse and Crémant de Wallonie (SM and Cr on Figure 1A), the coolest wine DPOs of Belgium. Intermediate values of the Huglin index are found in Vlaamse landwijn ("Vl" in Figure 1A).

Theoretical maturity for Chardonnay is considered to be reached on October 10th on average, 16 days later than in Champagne and 14 days later than in Jura (Table 3). In such conditions, earlier grapevine cultivars such as Sauvignon blanc (McIntyre *et al*., 1982; Parker *et al*., 2020) and/or sparkling wine (which require a lesser level of sugar content in grapes to be produced) could be preferred to avoid the risk of picking insufficiently ripe grapes for still wine production.

Spring frost appears as a major, if not the main challenge, for grapevine cultivation in Belgium (Table 3). Grapevine locations require sites on slopes where cold air accumulation is nil. Grapevine varieties providing late bud break should also be considered. Within early varieties, Sauvignon or Chasselas, two early varieties (McIntyre *et al*., 1982; Parker *et al*., 2020) with intermediate varieties (García de Cortázar-Atauri *et al*., 2009; McIntyre *et al*., 1982) could be more adapted than Chardonnay, which bud break is earlier.

TABLE 3. Comparison of the 2000–2020 average DOY of the phenological stages (Bud break, Flowering, Veraison, theoretical maturity) of the percentage of years with theoretical maturity of Chardonnay (200 g/L) reached before Oct. 30th and the percentage of the year with frost day after bud break simulated by MAR model forced by ERA5 reanalysis and averaged over the five regions currently planted with grapevines.

	Bud break DOY	Flowering DOY	Veraison DOY	Theoretical maturity (200g/L) DOY	% of years with theoretical maturity (200g/L) reached before Oct. 31th	Percentage of year with frost days after bud break (in %)
Bourgogne	104	162	227	256	100	24
Champagne	106	166	234	266	100	24
Jura	107	168	236	268	100	35
Alsace	106	163	227	255	100	20
Belgium Wine Region	112	173	246	282	100	49

Spring frost risks are highest in the easternmost parts of the country, where grapevines are little or not cultivated (Figure 5). By comparison, Hageland, Haspengouw and Côtes de Sambre et Meuse (Meuse valley more specifically) exhibit lower spring frost risk.

Extreme heat is not currently a risk for wine grape cultivation in Belgium. Together with limited temperature and sufficient precipitation during the growing season (Table 2), a little risk for heat and water stress is expected in Belgium vineyards. Precipitation during the growing season is sufficient yet not in excess, so that grapevine development should not be limited by rainfall. The western part of the country, together with Hageland and Haspengouw, exhibits lower precipitation amounts during the growing season than the eastern and southern parts of the country (Figure S3). The southernmost part of Crémant de Wallonie PDO is probably the most exposed region to grapevine spring diseases such as powdery and downy mildews, as rainfall and humidity are key variables of these diseases (Bois *et al*., 2017; Gadoury *et al*., 2012; Gessler *et al*., 2011).

CONCLUSIONS AND PERSPECTIVES

As the number of vineyards in Belgium has increased strongly over the last decade, we investigate here whether Belgium does have favourable climatic conditions for viticulture and what kind of climatic risks are currently present. Another question is whether Belgium shows similarities, from a climate point of view, with current wine-growing regions like the northernmost French regions. To address these questions, we use a regional climate model covering both the territory of Belgium and the eastern quarter of France to include the four wine regions of Champagne, Bourgogne, Jura and Alsace. The first analysis consists in evaluating the performance of the MAR concerning weather variables, bioclimatic indices and key dates of phenological stages against two observational networks regrouping more than 150 weather stations. In a second step, a more detailed comparison between the Belgian wine region and the aforementioned wine-growing regions is performed.

MAR simulations generally appear consistent with the observed data. However, they generally underestimate the maximum summer temperature over both domains, underestimate the minimum spring temperature over the Belgian domain, and overestimate the minimum spring temperature over the French domain. This bias leads to an underestimation of the Huglin index for both domains and an overestimation of the number of frost days after bud break in Belgium. However, the MAR model shows good performance in simulating the dates of the different phenological stages with respect to both the weather stations and the actual harvest dates in the field.

Although its precipitation amounts are comparable to the other regions, the Belgium wine region is clearly cooler according to both Huglin's index and spring frost occurrences. Nonetheless, when considering the biases of the MAR model, Belgium appears comparable to the four French regions concerning the mean spring temperature and it is comparable to Champagne and Jura concerning the mean summer temperatures. It seems to show a similar number of hot days, but the rareness of such events questions the robustness of this indicator. The simulation of the dates of the key phenological stages for the Chardonnay cultivar presents an excellent performance and are very close to the dates observed in the field. However, as the risk of frost after bud break remains much higher in Belgium, other cultivars could be considered to have a later bud break to avoid this spring frost.

The general conclusion of this work is, therefore, that the Belgian wine region meets climatic and bioclimatic criteria for the cultivation of grapevines. However, attention should be paid to frost days after bud break, which can be considered the biggest risk for wine production under present-day climate conditions.

A first perspective could be to analyse the sizable local differences that can be found, at terrain scales, according to the different topoclimates (Bonnefoy *et al*. (2013)). Here, we established that the Huglin index varies between 1500 and 1700 depending on the Belgian geographical regions. In future work, it is now needed to carry out a more detailed study in Belgium to assess the space and time variability of these key conditions that drive the phenology of the vines.

The focus could also be given to the potential ways to improve the reliability of the modelling chain through bias reduction. The present work does not propose to post-correct model outputs. The reasons are that, for this pilot study, we preferred to present results directly derived from a physics-based model. Besides, we have currently no reference observational dataset suited for the Belgium Wine Region. Current weather station networks are not optimal for assessing the climate diversity of the potential Belgian terroirs in line with their contrasted topography, vegetation, and soil features. Moreover, as the final goal of this study is to analyse the future climate evolution, post-correcting current model outputs would lead implicitly to assume that the biases are time-consistent, a hypothesis difficult to verify under a changing climate. Nevertheless, and in spite of these limitations, future work could attempt to use uni- or multivariate correction algorithms to facilitate the use of threshold-based indices, strongly sensitive to systematic model biases. This is especially critical for temperature or precipitation thresholds, two variables showing non-negligible errors and yet conveying key information for wine growing.

Another focus could be on the propagation of errors within the different atmospheric and phenological models used in this paper. Indeed, the errors produced by the different models used can add up and compensate for each other. It would therefore be interesting to reconstruct their pathways through three axes. The first one concerns the evaluation of errors between atmospheric models and atmospheric observations. The second is the evaluation of the errors between phenological models forced by atmospheric observations and

by atmospheric model simulations. A third evaluation could be conducted between the results of phenological models and what is actually observed in the field. This succession of control and evaluation of errors will allow us to determine the mode of propagation of errors between the different stages of this study.

Finally, another important issue concerns the long-term evolutions of these conditions and the potentialities for winemaking under ongoing climate change. Although it will have dramatic and prejudicial consequences for many regions (including Belgium, as illustrated notably by heat wave repetition (RMI, 2020) or the devastating floods that occurred during the summer of 2021 (Kreienkamp *et al.*, 2021)), climate change could probably open up new viticultural opportunities in cold regions, like Belgium (Jones and Schultz, 2016). Despite the projected warming trend, frost risk may not necessarily disappear or even significantly decrease, depending on local geographical and topographical conditions (Sgubin *et al*., 2018). To address these questions, we now plan to use the approach presented here (consisting of MAR simulations and climate-oriented and viticulture-oriented model output analyses) to downscale climate change projections from the Coupled Model Intercomparison Project phase 6 (CMIP6; Eyring *et al*., 2016). This work is mandatory to assess the long-term changing conditions and climate hazards that northern European vineyards (including Belgium) will undergo.

ACKNOWLEDGEMENTS

The authors thank Météo-France, especially Agnès Tamburini and Denis Thévenin, who provided the temperature and precipitation data, as part of an agreement with the University of Burgundy. The authors thank OGIMET webmaster for providing SYNOP observation over Belgium and France. Computational resources have been provided by the Consortium des Équipements de Calcul Intensif (CÉCI), funded by the Fonds de la Recherche Scientifique de Belgique (F.R.S.-FNRS) under Grant No. 2.5020.11 and by the Walloon Region.

REFERENCES

Anderson, K., & Aryal, N. R. (2013). *Which Winegrape Varieties are Grown Where? A Global Empirical Picture*. University of Adelaide Press. https://doi.org/10.20851/winegrapes

Baillod, M., & Baggiolini, M. (1993). *Les stades repères de la vigne*. *25*, 7–9.

Bois, B. (2019). Impacts on water availability for vitiviniculture worldwide using different potential evapotranspiration methods. *A Multidisciplinary Vision towards Sustainable Viticulture*, 44–48. https://ives-openscience.eu/4050/

Bois, B. (2020). Viticulture and climate: From global to local. *Proceedings of the 13th International Terroir Congress.*, 8.

Bois, B., Joly, D., Quénol, H., Pieri, P., Gaudillère, J.-P., Guyon, D., Saur, E., & van Leeuwen, C. (2018). Temperature-based zoning of the Bordeaux wine region. *OENO One*, *52*(4), Article 4. https://doi.org/10.20870/oeno-one.2018.52.4.1580

Bois, B., Zito, S., & Calonnec, A. (2017). Climate vs grapevine pests and diseases worldwide: The first results of a global survey. *OENO One*, *51*(2), 133–139. https://doi.org/10.20870/oeno-one.2017.51.2.1780

Bonhomme, M., Rageau, R., & Lacointe, A. (2010). Optimization of endodormancy release models, using series of endodormancy release data collected in France. *Acta Horticulturae*, *872*. https://doi.org/10.17660/ActaHortic.2010.872.4

Bonnefoy, C., Quenol, H., Bonnardot, V., Barbeau, G., Madelin, M., Planchon, O., & Neethling, E. (2013). Temporal and spatial analyses of temperature in a French wine-producing area: The Loire Valley. *International Journal of Climatology*, *33*(8), 1849–1862. https://doi.org/10.1002/joc.3552

Boulard, D., Castel, T., Camberlin, P., Sergent, A.-S., Bréda, N., Badeau, V., Rossi, A., & Pohl, B. (2016). Capability of a regional climate model to simulate climate variables requested for water balance computation: A case study over north-eastern France. *Climate Dynamics*, *46*(9–10), 2689–2716. https://doi.org/10.1007/s00382-015-2724-9

Doutreloup, S., Wyard, C., Amory, C., Kittel, C., Erpicum, M., & Fettweis, X. (2019). Sensitivity to Convective Schemes on Precipitation Simulated by the Regional Climate Model MAR over Belgium (1987–2017). *Atmosphere*, *10*(1), 34. https://doi.org/10.3390/atmos10010034

European Environment Agency (2014). *CLC2012 Addendum to CLC2006 Technical Guidelines* (EEA Technical Report) [Publication]. https://land.copernicus.eu/user-corner/technical-library/Addendum_finaldraft_v2_August_2014.pdf

Eyring, V., Bony, S., Meehl, G. A., Senior, C. A., Stevens, B., Stouffer, R. J., & Taylor, K. E. (2016). Overview of the Coupled Model Intercomparison Project Phase 6 (CMIP6) experimental design and organization. *Geoscientific Model Development*, *9*(5), 1937–1958. https://doi.org/10.5194/gmd-9-1937-2016

Ferguson, J. C., Tarara, J. M., Mills, L. J., Grove, G. G., & Keller, M. (2011). Dynamic thermal time model of cold hardiness for dormant grapevine buds. *Annals of Botany*, *107*(3), 389–396. https://doi.org/10.1093/aob/mcq263

Fettweis, X., Franco, B., Tedesco, M., van Angelen, J. H., Lenaerts, J. T. M., van den Broeke, M. R., & Gallée, H. (2013). Estimating the Greenland ice sheet surface mass balance contribution to future sea level rise using the regional atmospheric climate model MAR. *The Cryosphere*, *7*(2), 469–489. https://doi.org/10.5194/tc-7-469-2013

Fettweis, X., Wyard, C., Doutreloup, S., & Belleflamme, A. (2017). Noël 2010 en Belgique: Neige en Flandre et pluie en Haute-Ardenne. *Bulletin de La Société Géographique de Liège*, *68*, 97–107. https://doi.org/10.25518/0770-7576.4568

FGOV Economy (2021). *Un quart de viticulteurs belges en plus en 2020*. FOD Économie salle de presse, 27 mai 2021. http://news.economie.fgov.be/199451-un-quart-de-viticulteurs-belges-en-plus-en-2020

Fischer, E. M., & Schär, C. (2010). Consistent geographical patterns of changes in high-impact European heatwaves. *Nature Geoscience*, *3*(6), 398–403. https://doi.org/10.1038/ngeo866

Fraga, H., Atauri, I. G. de C., Malheiro, A. C., & Santos, J. A. (2016). Modelling climate change impacts on viticultural yield, phenology and stress conditions in Europe. *Global Change Biology*, *22*(11), 3774–3788. https://doi.org/10.1111/gcb.13382

Gadoury, D. M., Cadle-Davidson, L., Wilcox, W. F., Dry, I. B., Seem, R. C., & Milgroom, M. G. (2012). Grapevine powdery mildew (*Erysiphe necator*): A fascinating system for the study of the biology, ecology and epidemiology of an obligate biotroph. *Molecular Plant Pathology*, *13*(1), 1–16. https://doi.org/10.1111/j.1364-3703.2011.00728.x

García de Cortázar-Atauri, I., Brisson, N., & Gaudillere, J. P. (2009). Performance of several models for predicting budburst date of grapevine (*Vitis vinifera* L.). *International Journal of Biometeorology*, *53*(4), 317–326. https://doi.org/10.1007/s00484-009-0217-4

Gessler, C., Pertot, I., & Perazzolli, M. (2011). *Plasmopara viticola*: A review of knowledge on downy mildew of grapevine and effective disease management. *Phytopathologia Mediterranea*, *50*(1), 3–44. http://www.jstor.org/stable/26458675

Hall, A., & Jones, G. V. (2010). Spatial analysis of climate in winegrape-growing regions in Australia: Climate in winegrape growing regions in Australia. *Australian Journal of Grape and Wine Research*, *16*(3), 389–404. https://doi.org/10.1111/j.1755-0238.2010.00100.x

Hamdi, R., Giot, O., De Troch, R., Deckmyn, A., & Termonia, P. (2015). Future climate of Brussels and Paris for the 2050s under the A1B scenario. *Urban Climate*, *12*, 160–182. https://doi.org/10.1016/j.uclim.2015.03.003

Hersbach, H., Bell, B., Berrisford, P., Hirahara, S., Horányi, A., Muñoz-Sabater, J., Nicolas, J., Peubey, C., Radu, R., Schepers, D., Simmons, A., Soci, C., Abdalla, S., Abellan, X., Balsamo, G., Bechtold, P., Biavati, G., Bidlot, J., Bonavita, M., … Thépaut, J.-N. (2020). The ERA5 global reanalysis. *Quarterly Journal of the Royal Meteorological Society*, *146*(730), 1999–2049. https://doi.org/10.1002/qj.3803

Huglin, M. P. (1978). Nouveau mode d'évaluation des possibilités héliothermiques d'un milieu viticole. *Comptes Rendus de l'Académie d'Agriculture de France*, *64*, 1117.

Huglin, P., & Schneider, C. (1998). *Biologie et écologie de la vigne (2e éd.)* (Lavoisier). https://www.lavoisier.fr/livre/agriculture/biologie-et-ecologie-de-la-vigne-2e-ed/huglin/descriptif-9782743002602

IPCC (2021). Summary for Policymakers. [In: Masson Delmotte, V., Zhai, P., Pirani, A., Connors, S. L., Péan, C., Berger, S., Caud, N., Chen, Y., Goldfarb, L., Gomis, M. I., Huang, M., Leitzell, K., Lonnoy, E., Matthews, J. B. R., Maycock, T. K., Waterfield, T., Yelekçi, O., Yu, R., & Zhou, B. (2021) *Climate Change 2021: The Physical Science Basis. Contribution of Working Group I to the Sixth Assessment Report of the Intergovernmental Panel on Climate Change*.]

Jones, G. V., & Schultz, H. R. (2016). Climate change: Climate change and emerging cool climate wine regions. *Wine & Viticulture Journal, 31*(6), 51–53. https://search.informit.org/doi/10.3316/informit.523901697092406

Jones, G. V., White, M. A., Cooper, O. R., & Storchmann, K. (2005). Climate Change and Global Wine Quality. *Climatic Change*, *73*(3), 319–343. https://doi.org/10.1007/s10584-005-4704-2

Kittel, C. (2021). *Present and future sensitivity of the Antarctic surface mass balance to oceanic and atmospheric forcings: Insights with the regional climate model MAR* [PhD Thesis, Université de Liège, Liège, Belgique]. https://orbi.uliege.be/handle/2268/258491

Kittel, C., Amory, C., Agosta, C., Delhasse, A., Doutreloup, S., Huot, P.-V., Wyard, C., Fichefet, T., & Fettweis, X. (2018). Sensitivity of the current Antarctic surface mass balance to sea surface conditions using MAR. *The Cryosphere*, *12*(12), 3827–3839. https://doi.org/10.5194/tc-12-3827-2018

Kreienkamp, F., Philip, S. Y., Tradowsky, J. S., Kew, S. F., Lorenz, P., Arrighi, J., Belleflamme, A., Bettmann, T., Caluwaerts, S., Chan, S. C., Ciavarella, A., De Cruz, L., de Vries, H., Demuth, N., Ferrone, A., Fischer, rich M., Fowler, H. J., Goergen, K., Heinrich, D., ... Wanders, N. (2021). Rapid attribution of heavy rainfall events leading to the severe flooding in Western Europe during July 2021. *World Weather Atribution*. http://hdl.handle.net/1854/LU-8732135

Labbé, T., Pfister, C., Brönnimann, S., Rousseau, D., Franke, J., & Bois, B. (2019). Tehe longest homogeneous series of grape harvest dates, Beaune 1354–2018, and its significance for the understanding of past and present climate. *Climate of the Past*, *15*(4), 1485–1501. https://doi.org/10.5194/cp-15-1485-2019

van Leeuwen, C., & Darriet, P. (2016). The Impact of Climate Change on Viticulture and Wine Quality*. *Journal of Wine Economics*, *11*(1), 150–167. https://doi.org/10.1017/jwe.2015.21

Madelin, M., Bois, B., & Chabin, J.-P. (2010). Modification des conditions de maturation du raisin en Bourgogne viticole liée au réchauffement climatique. *EchoGéo*, *14*, Article 14. https://doi.org/10.4000/echogeo.12176

Malheiro, A. C., Santos, J. A., Fraga, H., & Pinto, J. G. (2010). Climate change scenarios applied to viticultural zoning in Europe. *Climate Research*, *43*(3), 163–177. https://doi.org/10.3354/cr00918

Marteau, R., Richard, Y., Pohl, B., Smith, C. C., & Castel, T. (2015). High-resolution rainfall variability simulated by the WRF RCM: Application to eastern France. *Climate Dynamics*, *44*(3–4), 1093–1107. https://doi.org/10.1007/s00382-014-2125-5

McIntyre, G. N., Lider, L. A., & Ferrari, N. L. (1982). The Chronological Classification of Grapevine Phenology. *American Journal of Enology and Viticulture*, *33*(2), 80–85.

Morales-Castilla, I., García de Cortázar-Atauri, I., Cook, B. I., Lacombe, T., Parker, A., van Leeuwen, C., Nicholas, K. A., & Wolkovich, E. M. (2020). Diversity buffers winegrowing regions from climate change losses. *Proceedings of the National Academy of Sciences of the United States of America*, *117*(6), 2864–2869. https://doi.org/10.1073/pnas.1906731117

Moriondo, M., Jones, G. V., Bois, B., Dibari, C., Ferrise, R., Trombi, G., & Bindi, M. (2013). Projected shifts of wine regions in response to climate change. *Climatic Change*, *119*(3), 825–839. https://doi.org/10.1007/s10584-013-0739-y

Nash, J. E., & Sutcliffe, J. V. (1970). River flow forecasting through conceptual models part I — A discussion of principles. *Journal of Hydrology*, *10*(3), 282–290. https://doi.org/10.1016/0022-1694(70)90255-6

Navrátilová, M., Beranová, M., Severová, L., Šrédl, K., Svoboda, R., & Abrhám, J. (2021). The Impact of Climate Change on the Sugar Content of Grapes and the Sustainability of their Production in the Czech Republic. *Sustainability*, *13*(1), 222. https://doi.org/10.3390/su13010222

Nesbitt, A., Kemp, B., Steele, C., Lovett, A., & Dorling, S. (2016). Impact of recent climate change and weather variability on the viability of UK viticulture – combining weather and climate records with producers' perspectives. *Australian Journal of Grape and Wine Research*, *22*(2), 324–335. https://doi.org/10.1111/ajgw.12215

Nikulin, G., Kjellström, E., Hansson, U., Strandberg, G., & Ullerstig, A. (2011). Evaluation and future projections of temperature, precipitation and wind extremes over Europe in an ensemble of regional climate simulations. *Tellus A*, *63*(1), 41–55. https://doi.org/10.1111/j.1600-0870.2010.00466.x

OIV (2021). *2020 statistical report on world vitiviniculture*.

Omazić, B., Telišman Prtenjak, M., Prša, I., Belušić Vozila, A., Vučetić, V., Karoglan, M., Karoglan Kontić, J., Prša, Ž., Anić, M., Šimon, S., & Güttler, I. (2020). Climate change impacts on viticulture in Croatia: Viticultural zoning and future potential. *International Journal of Climatology*, *40*(13), 5634–5655. https://doi.org/10.1002/joc.6541

Parker, A. K., Cortázar-Atauri, I. G. D., van Leeuwen, C., & Chuine, I. (2011). General phenological model to characterize the timing of flowering and veraison of *Vitis vinifera* L. *Australian Journal of Grape and Wine Research*, *17*(2), 206–216. https://doi.org/10.1111/j.1755-0238.2011.00140.x

Parker, A. K., García de Cortázar-Atauri, I., Gény, L., Spring, J.-L., Destrac, A., Schultz, H., Molitor, D., Lacombe, T., Graça, A., Monamy, C., Stoll, M., Storchi, P., Trought, M. C. T., Hofmann, R. W., & van Leeuwen, C. (2020). Temperature-based grapevine sugar ripeness modelling for a wide range of *Vitis vinifera* L. cultivars. *Agricultural and Forest Meteorology*, *285–286*, 107902. https://doi.org/10.1016/j.agrformet.2020.107902

Remenyi, T. A., Rollins, D. A., Love, P. T., Bindoff, N. L., & Harris, R. M. B. (2019). *Australia's Wine Future—A Climate Atlas*. University of Tasmania. http://climatefutures.org.au/category/technical-reports/

Resco, P., Iglesias, A., Bardají, I., & Sotés, V. (2016). Exploring adaptation choices for grapevine regions in Spain. *Regional Environmental Change*, *16*(4), 979–993. https://doi.org/10.1007/s10113-015-0811-4

Ridder, K. D., & Gallée, H. (1998). Land Surface–Induced Regional Climate Change in Southern Israel. *Journal of Applied Meteorology and Climatology*, *37*(11), 1470–1485. https://doi.org/10.1175/1520-0450(1998)037<1470:LSIRCC>2.0.CO;2

RMI (2020). *Rapport climatique 2020 de l'information aux services climatiques*. Royal Meteorological Institute of Belgium. https://www.meteo.be/uploads/media/5f7c66570cae5/fodb17-0001-raclimat2020-a4-fr-v6-web.pdf?token=/uploads/media/5f7c66570cae5/fodb17-0001-raclimat2020-a4-fr-v6-web.pdf

Seneviratne, S. I., Zhang X., M. Adnan, W. Badi, C. Dereczynski, A. Di Luca, S. Ghosh, I. Iskandar, J. Kossin, S., & Lewis, F. Otto, I. Pinto, M. Satoh, S. M. Vicente-Serrano, M. Wehner, B. Zhou. (2021). Weather and Climate Extreme Events in a Changing Climate. *In: Climate Change 2021: The Physical Science Basis. Contribution of Working Group I to the Sixth Assessment Report of the Intergovernmental Panel on Climate Change [Masson-Delmotte, V., P. Zhai, A. Pirani, S. L. Connors, C. Péan, S. Berger, N. Caud, Y. Chen, L. Goldfarb, M. I. Gomis, M. Huang, K. Leitzell, E. Lonnoy, J. B. R. Matthews, T. K. Maycock, T. Waterfield, O. Yelekçi, R. Yu and B. Zhou (Eds.)]*.

Sgubin, G., Swingedouw, D., Dayon, G., García de Cortázar-Atauri, I., Ollat, N., Pagé, C., & van Leeuwen, C. (2018). The risk of tardive frost damage in French vineyards in a changing climate. *Agricultural and Forest Meteorology*, *250–251*, 226–242. https://doi.org/10.1016/j.agrformet.2017.12.253

Termonia, P., Van Schaeybroeck, B., De Cruz, L., De Troch, R., Caluwaerts, S., Giot, O., Hamdi, R., Vannitsem, S., Duchêne, F., Willems, P., Tabari, H., Van Uytven, E., Hosseinzadehtalaei, P., Van Lipzig, N., Wouters, H., Vanden Broucke, S., van Ypersele, J.-P., Marbaix, P., Villanueva-Birriel, C., … Pottiaux, E. (2018). The CORDEX.be initiative as a foundation for climate services in Belgium. *Climate Services*, *11*, 49–61. https://doi.org/10.1016/j.cliser.2018.05.001

Tonietto, J., & Carbonneau, A. (2004). A multicriteria climatic classification system for grape-growing regions worldwide. *Agricultural and Forest Meteorology*, *124*(1–2), 81–97. https://doi.org/10.1016/j.agrformet.2003.06.001

Wang, E., & Engel, T. (1998). Simulation of phenological development of wheat crops. *Agricultural Systems*, *58*(1), 1–24. https://doi.org/10.1016/S0308-521X(98)00028-6

Wyard, C., Scholzen, C., Doutreloup, S., Hallot, É., & Fettweis, X. (2021). Future evolution of the hydroclimatic conditions favouring floods in the south-east of Belgium by 2100 using a regional climate model. *International Journal of Climatology*, *41*(1), 647–662. https://doi.org/10.1002/joc.6642

Xu, Y., Castel, T., Richard, Y., Cuccia, C., & Bois, B. (2012). Burgundy regional climate change and its potential impact on grapevines. *Climate Dynamics*, *39*(7), 1613–1626. https://doi.org/10.1007/s00382-011-1284-x